



Improvement in electrical and energy storage properties of lead-free BNKT-BT piezoceramics

Manlika KAMNOY¹, Supalak MANOTHAM², Pichitchai BUTNOI², Sukum EITSSAYEAM¹, and Piewpan PARJANSRI^{3,*}

¹ Department of Physics and Materials Science, Faculty of Science, Chiang Mai University, Chiang Mai 50200, Thailand

² Department of Metallurgical Technology, Faculty of Technical Education, Rajamangala University of Technology Krungthep, Bangkok 10120, Thailand

³ Physics Division, Faculty of Science and Technology, Rajamangala University of Technology Krungthep, Bangkok 10120, Thailand

*Corresponding author e-mail: piewpan.p@mail.rmutk.ac.th

Received date:

26 February 2025

Revised date:

7 May 2025

Accepted date:

16 June 2025

Keywords:

Lead-free piezoelectric;

Dielectric constant;

Energy storage;

BNKT-BT ceramic

Abstract

The electrical characteristics and energy storage performance of BNKT-BT lead-free piezoceramics were examined. All ceramics were produced via the mixed oxide technique. The findings indicated that the density of this ceramic system varied between 5.61 and 5.83 g·cm⁻³. Conditions with 2.0 mol% (BT=0.02) and 6.0 mol% (BT=0.06) exhibited the largest dielectric constant (ϵ_r) at both ambient temperature and elevated temperature, with values of 1307 and 4272, respectively. The ceramic sample with BT = 0.06 exhibited the highest values of %strain ~0.13 and a $d_{33}^* \sim 179.65$ pm·V⁻¹. Furthermore, BT-doped ceramics yielded optimal energy storage densities compared to undoped BNKT ceramics. The sample containing 4.0 mol% (BT=0.04) reached the maximum energy storage density ($W \sim 0.31$ J·cm⁻³) with an energy storage efficiency ($\eta \sim 37.89\%$).

1. Introduction

Lead-based piezoceramics materials are useful for many applications such as actuators, sensors, and energy harvesting devices [1] because they have special properties that convert mechanical stress into electrical energy. Moreover, their excellent piezoelectric and dielectric properties. However, the volatility of Pb oxide during the high-temperature process affects environmentally friendly. As a result, many researchers are considering replacing lead-based materials with lead-free ceramics. Lead-free materials have recently been discovered, particularly for energy storage and harvesting applications. Bismuth sodium titanate (BNT) ceramics are among the most promising and competitive ecologically sustainable ferroelectric materials for energy storage. They have a high Curie temperature ($T_C \sim 320^\circ\text{C}$), elevated dielectric constant (ϵ_r), and stability at elevated temperatures [2-5]. Nevertheless, the energy storage density (W_{rec}) observed in pure BNT ceramic is very low [6]. Other perovskite materials are commonly added to BNT-based devices to enhance their mechanical and electrical capabilities. BaTiO₃ (BT) is a common practice to improve piezoelectric performance, dielectric, and energy storage properties [7-9]. The BNKT-based ferroelectric is one of the most researched lead-free piezoelectric ceramics due to its large spontaneous polarization [9,10]. Moreover, it shows that dielectric properties with a broad temperature range, low dielectric loss ($\tan\delta$), and high permittivity (ϵ_r) may provide exceptional energy storage properties for applications [11,12]. It is

widely recognized that pure BNKT ceramic is inadequate for energy storage because of its elevated high polarization (P_r). Recently, researchers have focused on refining the composition, microstructure, and doping techniques of BNKT ceramics to improve their energy storage performance, making them ideal for high-performance energy storage applications. The incorporation of additional oxides and compounds is reported to enhance the dielectric characteristics, piezoelectric properties, and energy storage capabilities of BNKT ceramics such as BNKT-ZnO [13], BNKT-BT [14], and BNKT-xBMN [15,16], BNKT-BiAlO₃ [17].

Thus, this work investigates the electrical characteristics and energy storage performance of lead-free piezoceramics Bi_{0.5}Na_{0.4}K_{0.1}TiO₃-BaTiO₃ (BNKT-BT). This research attempts to solve the issues related to energy density, dielectric constant, and overall efficiency of lead-free materials by altering the composition and improving fabrication conditions.

2. Experimental

In this study, (1-x)Bi_{0.5}Na_{0.4}K_{0.1}TiO₃-xBaTiO₃ (BNKT-xBT) ceramics (x = 0 mol% to 8 mol%) were produced via the solid-state reaction process. The Bi₂O₃ (≥99.9%), NaCO₃ (99.95% to 100.5%), K₂CO₃ (99.95% to 100.5%), and TiO₂ (99% to 105.5%) starting granules were weighed and combined with alcohol. The composite powder was subjected to ball milling for 24 h and then calcined at

900°C for 2 h. The powder was subsequently combined with binder, and formed into pellets. Then, they were sintered at 1100°C for 2 h.

X-ray diffraction (XRD) was employed to analyze the phase formation of the bulk ceramic systems. To investigate the electrical characterizations, ceramics were coated with silver material to create an electrode. The automatic dielectric measurement apparatus (Agilent Technologies) was used to measure the dielectric characterization. An electric field of up to $7 \text{ kV} \cdot \text{mm}^{-1}$ was applied to the electrode-coated samples to measure their ferroelectric properties (Radiant Technology Inc.). The ferroelectric parameters, including remnant polarization (P_r), coercive fields (E_c), and P–E loop, were plotted with the BT content. Using the Radiant ferroelectric system in conjunction with an optical displacement sensor, the strain-electrical field was examined to ascertain the butterfly strain curve.

3. Results and discussion

Figure 1 displays the X-ray diffraction (XRD) patterns of BNKT-BT ceramic. The detected diffraction peaks correspond to the (100), (110), (111), (002), (200), (210), and (211) crystal planes (this is a JC-file standard). This indicates that the BNKT-BT ceramics formed a perovskite phase for all compositions, ranging from x (BT) = 0.00 to x (BT) = 0.08. The XRD patterns demonstrate a consistent shift in peak positions as BT content is added, especially in the (110) planes. This change indicates a distortion in the lattice resulting from incorporating Ba and Ti ions into the BNKT matrix, which changes the crystal structure of the BNKT ceramics [18,19]. The ionic radius of Ba^{2+} (1.61 Å) exceeds that of Bi^{3+} (1.03 Å), whereas Ti^{4+} (0.605 Å) is less than Nb^{5+} (0.64 Å) and K^{+} (1.38 Å) within the BNKT structure. The increase in BT content leads to an expansion of the lattice as Ba^{2+} is incorporated, resulting in larger lattice parameters and a shift of the peaks towards a lower angle. The lattice expansion induces structural distortions that can influence the piezoelectric ferroelectric, and dielectric properties of BNKT ceramics. In the non-BT sample compositions, the peaks exhibited a rhombohedral (R) phase, evidenced by the splitting peaks around $2\theta \sim 40^\circ$ to 42° for the (111) plane and a singular peak at $2\theta \sim 46^\circ$ to 48° for the (200) plane. Conversely, the XRD peaks of BT-added samples ($x \geq 2 \text{ mol\%}$) revealed a tetragonal phase, characterized by the splitting peak of (200) reflections and a singular peak at (111) plane. This signifies that the crystal structure of BNKT transitions to a tetragonal phase upon the addition of BT [20-22].

The Archimedes principle approach was used to determine the density of all ceramics. The density value decreased with increasing BT content which was in the range of $5.61 \text{ g} \cdot \text{cm}^{-3}$ to $5.82 \text{ g} \cdot \text{cm}^{-3}$, as indicated in Table 1. Figure 2 indicates the dielectric constant (ϵ_r) and

dielectric loss ($\tan\delta$) as a function of frequency in the range of 1 kHz to 100 kHz. It was found that the dielectric constant significantly changed with frequency and BT content. The $\tan\delta$ value is stable with a frequency range of 1 kHz to 100 kHz observed for the BT-added samples. In contrast, the non-BT sample shows an increase in the dielectric loss at high frequencies. Furthermore, the dielectric constant decreases with frequency may indicate that ceramic systems exhibit relaxor behavior [23]. The dielectric constant was between 917 and 1307 at ambient temperature. The dielectric constant increased when the BT content was increased to 2 mol%. Subsequently, the values decreased as the BT content increased continuously from 4 mol% to 8 mol%. The results of this investigation are consistent with those of Vuong *et al.* [14].

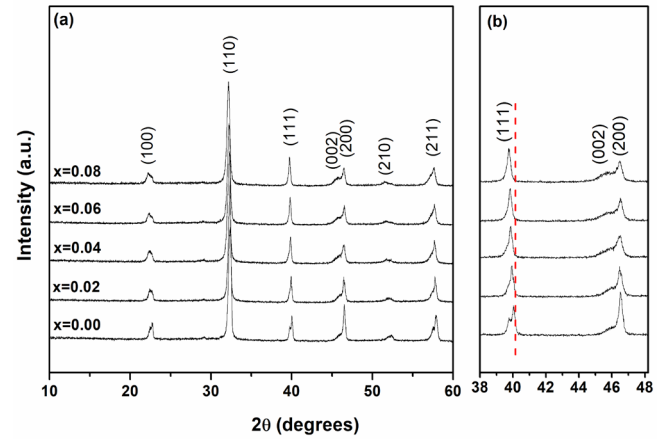


Figure 1. X-ray diffraction (XRD) patterns of BNKT-BT ceramics.

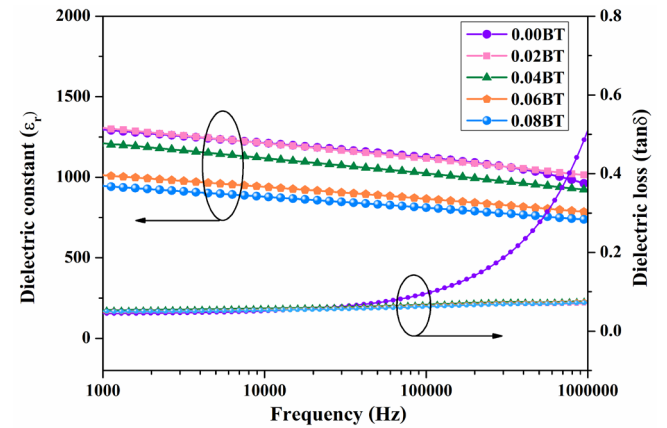


Figure 2. Dielectric constant (ϵ_r) and dielectric loss ($\tan\delta$) as a function of frequency measured at room temperature.

Table 1. Density values and dielectric properties of BNKT-xBT ceramics.

Samples	Density [$\text{g} \cdot \text{cm}^{-3}$]	T_{room}		T_{max}		T_m [°C]	T_{F-R} [°C]
		ϵ_r	$\tan\delta$	ϵ_r	$\tan\delta$		
0.00	5.82	1296	0.045	4071	0.041	301	118
0.02	5.76	1307	0.051	4196	0.044	294	152
0.04	5.75	1209	0.053	4168	0.038	290	158
0.06	5.68	1012	0.048	4272	0.044	289	200
0.08	5.61	946	0.051	4206	0.044	283	215

T_{room} is the sample measured at room temperature, and T_{max} is the sample measured at a high temperature.

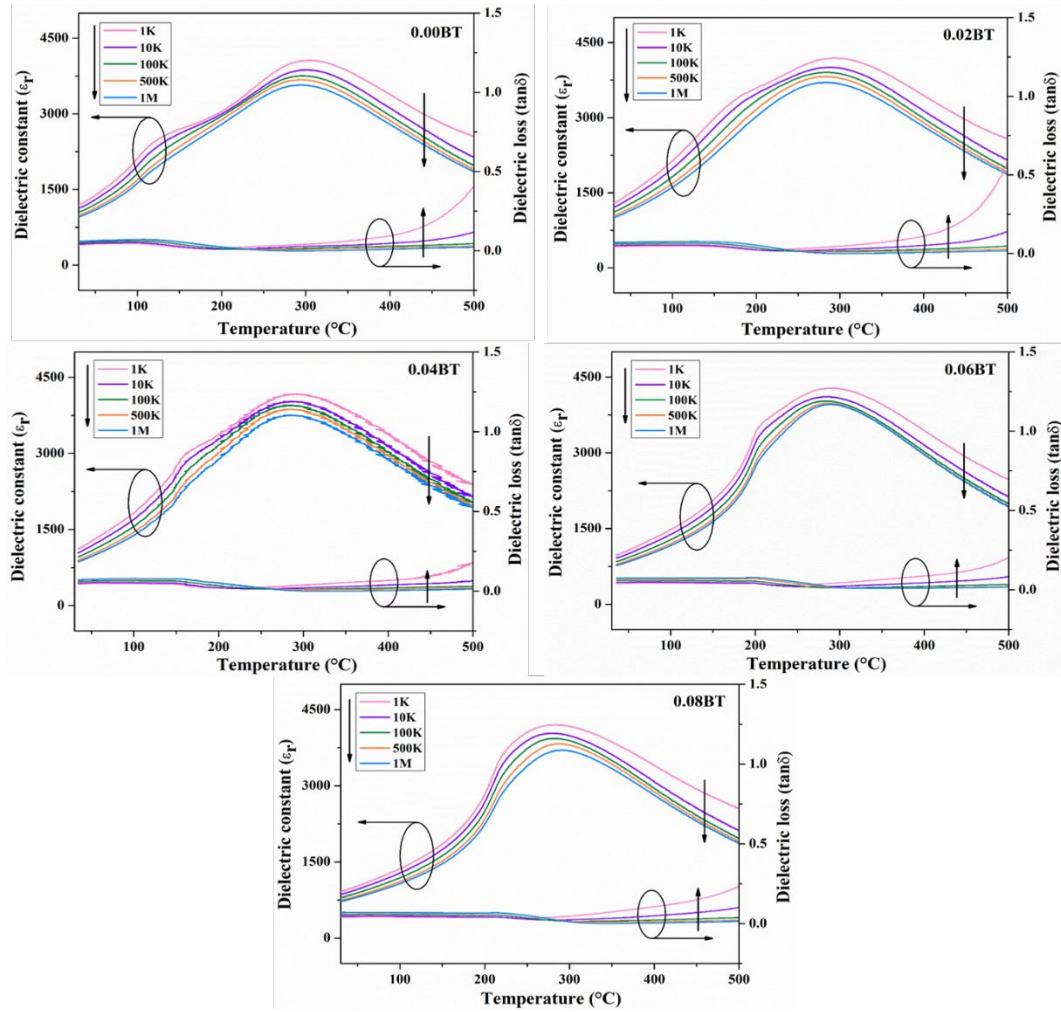


Figure 3. Dielectric constant (ϵ_r) and dielectric loss ($\tan\delta$) as a function of temperatures for NBKT-BT ceramics.

Figure 3 illustrates the dielectric characteristics measured at elevated temperatures, with the values enumerated in Table 1. The results indicate that BNKT-BT ceramic demonstrated diffusion phase transition behavior characterized by two dielectric peaks. Simultaneously, the $\tan\delta$ of BNKT at low temperatures and high frequencies is consistently low across all samples. Figure 3 illustrates that the dielectric peaks exhibit an initial shoulder peak at low temperatures (approximately 100°C to 200°C), corresponding to the transition from the ferroelectric to the ergodic relaxor phase state (T_{F-R}), and a second peak at a maximum temperature (approximately 300°C), indicative of the transition from the ferroelectric to the paraelectric phase state (T_m) [20,24,25].

The dielectric constant shows a typical relaxor-like behavior for all compositions, as evident from the broadening of the dielectric peaks and the frequency dependence of T_{max} . The findings indicate that the ceramics had a relaxor ferroelectric state [26]. In addition, it can be seen that T_m shifts to lower temperatures with increasing BT content from 301°C for the non-BT sample ($x=0$) to 283°C for the BT-added samples (refer to Table 1), consistent with improved thermal stability. A slight increase in dielectric loss is observed near the maximum temperature, particularly at lower frequencies, which can be attributed to increased dipolar relaxation and domain wall motion at elevated temperatures. From Table 1, the dielectric constant (ϵ_r) at maximum temperature (T_m) increased when BT was added. The dielectric constant

reaches its maximum at the Curie temperature (T_{max}) of 4272 obtained at 0.06BT sample. This result indicates that BT doping enhances the dielectric response of BNKT ceramic. This behavior could be due to increased dipole interactions and domain wall mobility with BT doping. The dielectric loss ($\tan\delta$) remains relatively stable across all frequencies and compositions. The ferroelectric hysteresis loops (P-E loops) of BNKT-BT ceramics are shown in Figure 4. The result was found that the P-E loop behavior shows a normal ferroelectric hysteresis loop and the area enclosed by the loops slim with increasing BT content, indicating reduced energy loss. The remnant polarization (P_r) values and maximum polarization (P_{max}) decrease with increasing BT content (seen in Table 2). The inclusion of BT substantially disrupts the long-range ferroelectric order of the BNKT-based system, resulting in an increased degree of ergodicity [27]. The coercive field (E_c) values decrease from 34.5 for the non-BT sample to 21.5 for the sample of 0.4BT. After that, it increases as the amount of BT increases. The P-E hysteresis loops also provide insights into the energy storage characterization of BNKT-BT ceramics. From the ferroelectric properties result, it can be noted that adding BT improves energy storage properties which is observed with the result of $P_{max}-P_r$. Table 2 presents the energy storage efficiency (η) and energy storage density (W) of BNKT-BT ceramics. The W and η values were derived from the hysteresis loop utilizing the subsequent Equation (1-2) [28,29].

$$W = \int_{P_r}^{P_{max}} E dp \quad (1)$$

$$\eta = \frac{W}{W + W_{loss}} \quad (2)$$

where W denotes the energy storage density, P_{max} and P_r denote maximum and remnant polarization, respectively, E refers to the applied electric field and W_{loss} refers to the energy loss density. The area of the P-E hysteresis loops was integrated to get the energy loss density (W_{loss}) and energy storage density (W) of ceramics. The highest energy storage density recorded at the compositions of 0.02BT and 0.04BT indicates that these concentrations are suitable for enhancing energy storage efficiency in these ceramics. Additionally, the breakdown field (E_c) decreases with BT doping, enhancing energy storage capabilities.

The electric-induced bipolar strain (S-E loop) of BNKT-BT ceramics investigated under an electric field of $70 \text{ kV} \cdot \text{cm}^{-1}$ is illustrated in Figure 5(a). The findings show that the S-E loops of BNKT ceramic systems exhibit no substantial variation concerning BT content. The S-E loops of all ceramics exhibit a “butterfly shape”, a typical feature of FE ferroelectric materials (normal ferroelectric), characterized by approximately negative strain (S_{neg}). The rising BT concentration of $x = 2 \text{ mol\%}$ signifies distinct S-E loops with a minor S_{neg} compared to other compositions. The decrease in S_{neg} for BNKT samples with additional BT may result from the transformation of ferroelectric domains into dynamically active nano-domains in the ergodic relaxor state [30]. The maximal strain (S_{max}) and the normalized strain coefficient d^*_{33} (derived using the equation S_{max}/E_{max}) are illustrated in Figure 5(b) and listed in Table 2. The results indicate that the S_{max} and d^*_{33} values diminished with BT content at $x = 2 \text{ mol\%}$ and $x = 4 \text{ mol\%}$, followed by a further rise in BT content at $x = 6 \text{ mol\%}$, and subsequently

dropped at the sample with 8.0 mol% BT. The S_{max} and d^*_{33} attain peak values of 0.13% and $179.65 \text{ pm} \cdot \text{V}^{-1}$, respectively, for the sample with $x = 6 \text{ mol\%}$ BT. It is commonly acknowledged that both intrinsic factors (e.g., lattice structure) and external factors (e.g., mechanisms of domain wall motion) contribute to electric field-induced strain. The increase in strain for $x = 0.06$ might be due to a higher level of ergodicity, leading to the maximum strain and a lower negative strain value relative to the undoped BNKT sample. Additionally, the sample with this doping showed high S_{max} and low S_{neg} , likely due to the way ergodic and non-ergodic relaxor phases interact. Furthermore, the decrease in the P_r value along with a change in the shape of the hysteresis loop results in a large electric field-induced strain. [29,31].

The piezoelectric charge coefficient (d_{33}) and the piezoelectric voltage coefficient (g_{33}) are detailed in Table 2. The results indicate that the piezoelectric coefficients (d_{33}) tended to decrease with increasing BT content. The decrease in d_{33} values for BT-added samples might be due to the decrease in P_r value. Nonetheless, an additional rise in BT content over this threshold results in a deterioration in piezoelectric performance due to the destabilization of the ferroelectric phase and the emergence of relaxor-like behavior.

The g_{33} values were ascertained via Equation (3) [32]:

$$g_{33} = \frac{d_{33}}{\epsilon_r \epsilon_0} \quad (3)$$

When ϵ_0 is the relative concession or dielectric constant of the vacuum. ϵ_r is the dielectric constant of the material at room temperature. According to the calculations, the g_{33} value of BNKT-BT ceramics was $9.40 \text{ Vm} \cdot \text{N}^{-1}$ to $13.24 (\times 10^{-3}) \text{ Vm} \cdot \text{N}^{-1}$. The maximum value of g_{33} was found in ceramic specimens added with BT in the content of 8.0 mol%.

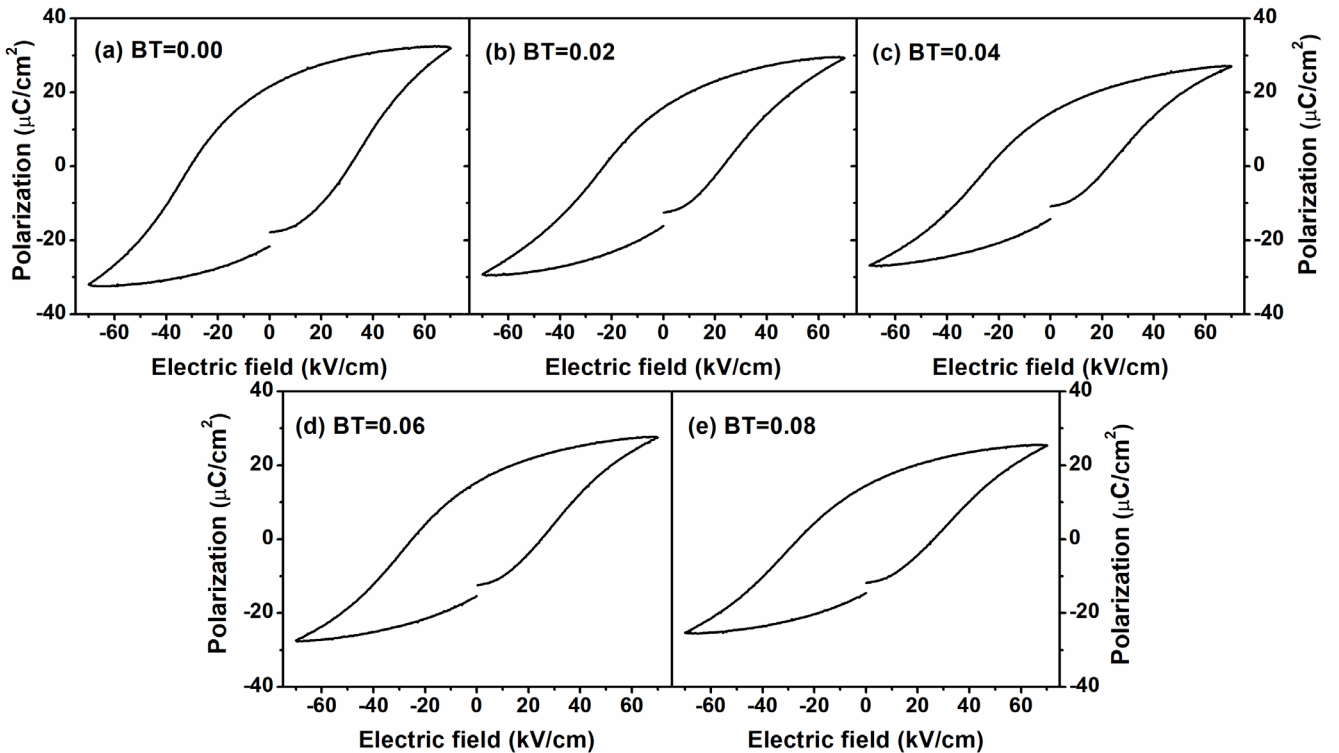


Figure 4. P-E hysteresis loops of BNKT-BT ceramics.

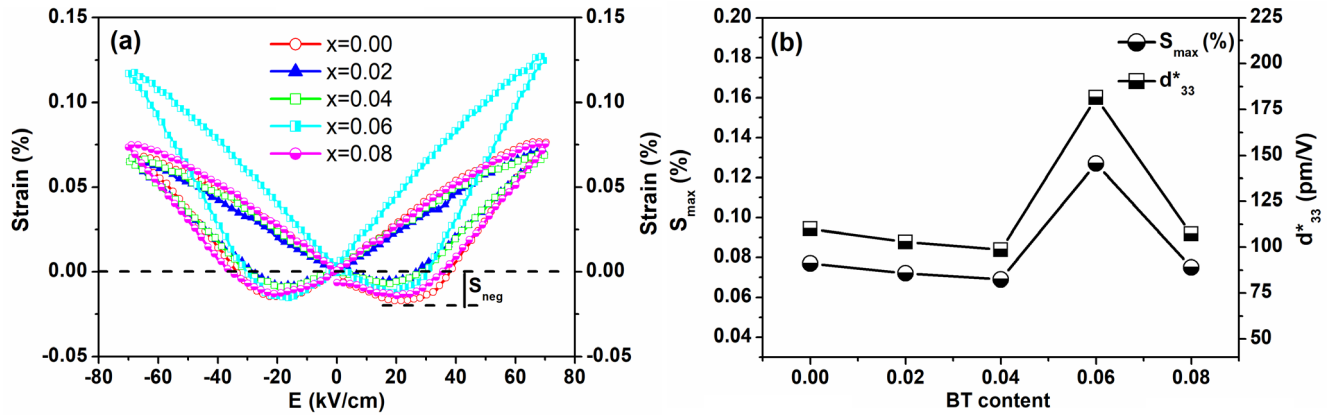


Figure 5. (a) S-E hysteresis loops and (b) plots of S_{max} and d_{33}^* values of BNKT-BT ceramics.

Table 2. Summary of ferroelectric, piezoelectric, and energy storage properties for BNKT-BT ceramics.

Samples	P_r [$\mu\text{C}\cdot\text{cm}^{-2}$]	P_{max} [$\mu\text{C}\cdot\text{cm}^{-2}$]	$P_{max}-P_r$ [$\mu\text{C}\cdot\text{cm}^{-2}$]	S_{max} [%]	d_{33} [$\text{pC}\cdot\text{N}^{-1}$]	d_{33}^* [$\text{pm}\cdot\text{V}^{-1}$]	g_{33} [$10^{-3}\text{ Vm}\cdot\text{N}^{-1}$]	W_{rec} [$\text{J}\cdot\text{cm}^{-3}$]	η [%]
0.00	21.4	32.3	6.60	0.08	123.7	110.17	10.78	0.22	16.83
0.02	16.0	29.3	13.3	0.07	108.8	104.50	9.40	0.31	32.26
0.04	15.0	27.0	12.0	0.07	105.3	102.40	9.84	0.31	37.89
0.06	15.5	27.6	12.1	0.13	101.7	179.65	11.35	0.29	31.46
0.08	14.5	25.3	10.8	0.08	110.9	104.17	13.24	0.25	27.33

4. Conclusions

A solid-state reaction process completely synthesized BNKT-BT ceramics. The XRD investigation verifies that the BNKT-BT ceramics retain a perovskite structure throughout all compositions. The dielectric constant of BNKT ceramics improves with BT doping. The optimal composition for achieving a high dielectric constant at room and maximum temperature appears to be at 2.0 mol% BT and 8.0 mol% BT, respectively. The maximum values of S_{max} and d_{33}^* of 0.13% and $179.65\text{ pm}\cdot\text{V}^{-1}$, respectively were achieved for the sample with $x = 6.0\text{ mol}\%$ BT. A high energy storage density $W_{rec} \sim 0.31\text{ J}\cdot\text{cm}^{-3}$ was attained in the sample with $x = 2.0\text{ mol}\%$ and $4.0\text{ mol}\%$ BT. These results suggest that tailored BT doping can effectively improve the performance of BNKT lead-free piezoceramics, making them suitable for advanced energy storage and piezoelectric applications.

Acknowledgments

The authors thank the Rajamangala University of Technology Krungthep, part of the Research and Development Institute and Faculty of Science and Technology for their financial support. Chiang Mai University provided partial support for this study.

References

- [1] Z. L. Wang, and J. Song, "Piezoelectric nanogenerators based on zinc oxide nanowire arrays," *Science*, vol. 312, pp. 242-246, 2006.
- [2] G. A. Smolensky, "New ferroelectrics of complex composition IV," *Soviet physics. Solid state*, vol 2, p. 2651, 1961.
- [3] H. Nagata, T. Shinya, Y. Hiruma, T. Takenaka, I. Sakaguchi, and H. Haneda, "Piezoelectric properties of bismuth sodium titanate ceramics," *Ceramic Transactions*, vol 167, p. 213, 2005.
- [4] T. Takenaka, K.O. Sakata, and K. O. Toda, "Piezoelectric properties of $(\text{Bi}_{1/2}\text{Na}_{1/2})\text{TiO}_3$ -based ceramics," *Ferroelectrics*, vol. 106, no. 1, p. 375, 1990.
- [5] W. Zhu, Z.-Y. Shen, W. Deng, K. Li, W. Luo, F. Song, X. Zeng, Z. Wang, and Y. Li, "A review: $(\text{Bi}, \text{Na})\text{TiO}_3$ (BNT)-based energy storage ceramics," *Journal of Materiomics*, vol. 10, no. 1, pp. 86-123, 2024.
- [6] M. Benyoussef, M. Zannen, J. Belhadi, M. Bouchaib, J.L. Dellis, and M.E. Marssi, "Dielectric, ferroelectric, and energy storage properties in dysprosium doped sodium bismuth titanate ceramics," *Ceramic International*, vol. 44, no. 16, pp. 19451-19460, 2018.
- [7] Q. Li, C. Zhou, J. Xu, L. Yang, X. Zhang, and W. Zeng, "Tailoring antiferroelectricity with high energy-storage properties in $\text{Bi}_{0.5}\text{Na}_{0.5}\text{TiO}_3$ - BaTiO_3 ceramics by modulating Bi/Na ratio," *Journal of Materials Science Materials in Electronics*, vol. 27, p. 10810, 2016.
- [8] T. Badapanda, S. Sahoo, and P. Nayak, "Dielectric, ferroelectric and piezoelectric study of BNT-BT solid solutions around the MPB region," *IOP Conference Series: Materials Science and Engineering*, vol. 178, no. 1, 2017.
- [9] Z. Yang, B. Liu, and Y. Hou, "Structure and electrical properties of $(1-x)\text{Bi}_{0.5}\text{Na}_{0.5}\text{TiO}_3$ - $x\text{Bi}_{0.5}\text{K}_{0.5}\text{TiO}_3$ ceramics near morphotropic phase boundary," *Materials research bulletin*, vol. 43, pp. 81-89, 2008.
- [10] R. Sumang, T. Bongkarn, and N. Kumar, "Investigation of a new lead-free $(1-x)\text{BNT}$ - $x\text{BKT}$ - $y\text{BZT}$ piezoelectric ceramics," *Ceramic International*, vol. 43, pp. S102-S109, 2017.

- [11] H. Yang, F. Yan, and Y. Lin, "Lead-free BaTiO₃-Bi_{0.5}Na_{0.5}TiO₃-Na_{0.73}Bi_{0.09}NbO₃ relaxor ferroelectric ceramics for high energy storage," *Journal of the European Ceramic Society*, vol. 37, pp. 3303-3311, 2017.
- [12] X. Ren, L. Jin, and Z. Peng, "Regulation of energy density and efficiency in transparent ceramics by grain refinement," *Chemical Engineering Journal*, vol. 390, p.124566, 2020.
- [13] P. Jaita, K. Saenkam, and G. Rujijanagul, "Improvements in piezoelectric and energy harvesting properties with a slight change in depolarization temperature in modified BNKT ceramics by a simple technique," *RSC Advances*, vol. 13, pp. 3743-3758, 2023.
- [14] L.D. Vuong, and P.D. Gio, "Enhancement in dielectric, ferroelectric, and piezoelectric properties of BaTiO₃-modified Bi_{0.5}(Na_{0.4}K_{0.1})TiO₃ lead-free ceramic," *Journal of Alloys and Compounds*, vol. 817, p. 152790, 2020.
- [15] H-l. Lian, X-j. Liang, M-n. Shi, L-n. Liu, and X-m. Chen. "Improved dielectric temperature stability and energy storage properties of BNT-BKT-based lead-free ceramics," *Ceramic International*, vol. 50, no. 3, pp. 5021-5031, 2024.
- [16] Z. Peng, J. Wang, M. Niu, X. Nie, S. Xu, F. Zhang, J. Wang, D. Wu, Z. Yang, and X. Chao, "Structure, electrical properties and energy storage performance of BNKT-BMN ceramics," *Journal of Materials Science Materials in Electronics*, vol. 33, pp. 3053-3064, 2022.
- [17] Z. Yu, Y. Liu, and M. Shen, "Enhanced energy storage properties of BiAlO₃ modified Bi_{0.5}Na_{0.5}TiO₃-Bi_{0.5}K_{0.5}TiO₃ lead-free antiferroelectric ceramics," *Ceramic International*, vol. 43, pp. 653-7659, 2017.
- [18] N. Chen, W. Yao, C. Liang, S. Xiao, J. Hao, Z. Xu, and R. Chu, "Phase structure, ferroelectric properties, and electric field-induced large strain in lead-free 0.99[(1-x)(Bi_{0.5}Na_{0.5})TiO₃-x(Bi_{0.5}K_{0.5})TiO₃]-0.01Ta piezoelectric ceramics," *Ceramic International*, vol. 42, p. 9660, 2016.
- [19] X. Wang, H. Gao, X. Hao, and X. Lou, "Enhanced piezoelectric, electrocaloric and energy storage properties at high temperature in lead-free Bi_{0.5}(Na_{1-x}K_{x0.5})TiO₃ ceramics," *Ceramic International*, vol. 45, p. 4274, 2019.
- [20] T. Takenaka, K. Maruyama, and K. Sakata, (Bi, Na)TiO₃-BaTiO₃ system for lead-free piezoelectric ceramics. *Japanese Journal of Applied Physics*, vol. 30, p. 2236, 1991.
- [21] J. Y. Ha, J. W. Choi, C. Y. Kang, D. J. Choi, H. J. Kim, and S. J. Yoon, *Materials Chemistry and Physics*, vol. 90, p. 396, 2005.
- [22] J. Wu, D. Xiao, W. Wu, Q. Chen, J. Zhu, Z. Yang, and J. Wang, "Role of room-temperature phase transition in the electrical properties of (Ba, Ca)(Ti, Zr)O₃ ceramics," *Scripta materialia*, vol. 65, p. 771, 2011.
- [23] M. Promsawat, A. Watcharapasorn, and S. Jiansirisomboon, "Effects of ZnO nanoparticulate addition on the properties of PMNT ceramics," *Nanoscale Research Letters*, vol. 7, p. 65, 2012.
- [24] Y. Li, W. Chen, J. Zhou, Q. Xu, H. Sun, and R. Xu, "Dielectric and piezoelectric properties of lead-free (Na_{0.5}Bi_{0.5})TiO₃-NaNbO₃ ceramics," *Materials Science and Engineering: B*, vol. 112, p. 5, 2004.
- [25] K. Sakata, and Y. Masuda, "Ferroelectric and antiferroelectric properties of (Na_{0.5}Bi_{0.5})TiO₃-SrTiO₃ solid solution ceramics," *Ferroelectrics*, vol. 7, p. 347, 1974.
- [26] V. V. Shvartsman, and D. C. Lupascu, "Lead-free relaxor ferroelectrics," *Journal of the American Ceramic Society*, vol. 95, p. 1, 2012.
- [27] G. Hao, W. Bai, W. Li, B. Shen, and J. Zhai, "Phase transitions, relaxor behavior, and large strain response in LiNbO₃-modified Bi_{0.5}(Na_{0.80}K_{0.20})_{0.5}TiO₃ lead-free piezoceramics," *Journal of Applied Physics*, vol. 114, p. 044103, 2013.
- [28] A. Chauhan, S. Patel, and R. Vaish, "Mechanical confinement for improved energy storage density in BNT-BT-KNN lead-free ceramic capacitors," *AIP Advances*, vol. 4, p. 087106, 2014.
- [29] R. A. Malik, A. Hussain, A. Maqbool, A. Zaman, T. K. Song, W. J. Kim, and M. H. Kim, "Giant strain, thermally-stable high energy storage properties and structural evolution of Bi-based lead-free piezoceramics," *Journal of Alloys and Compounds*, vol. 682, p. 302, 2016.
- [30] A. Zaman, Y. Iqbal, A. Hussain, M. H. Kim, and R. A. Malik, "Dielectric, ferroelectric, and field-induced strain properties of Ta-doped 0.99Bi_{0.5}(Na_{0.82}K_{0.18})_{0.5}TiO₃-0.01LiSbO₃ ceramics," *Journal of Materials Science*, vol. 49, p. 3205, 2014.
- [31] X. Zhou, G. Xue, H. Luo, C.R. Bowen, and D. Zhang, "Phase structure and properties of sodium bismuth titanate lead-free piezoelectric ceramics," *Progress in Materials Science*, vol 122, p. 100836, 2021.
- [32] J. Moulson, and J.M. Herbert, "Electroceramics materials, properties, applications," 2nd ed., New York: Wiley, 2003.